Cuadernos de Investigación Geográfica *Geographical Research Letters*	2025	Nº 51 (1)	pp. 33-49	EISSN 1697-9540

Copyright © 2025, The authors. This work is licensed under a Creative Commons Attribution 4.0 International License.

http://doi.org/10.18172/cig.6337

EFFECTS OF DEM RESOLUTION AND AREA THRESHOLDS ON AUTOMATED FLUVIAL MORPHOMETRY, ARROYO DEL ORO (ARGENTINA)

ANA CASADO[1]*,
FEDERICO JAVIER BERÓN DE LA PUENTE[2],
VERÓNICA GIL[2]

[1]*Consejo Nacional de Investigaciones Científicas y Técnicas (CONICET), Centro de Emprendedorismo y Desarrollo Territorial Sostenible, Universidad Provincial del Sudoeste, Argentina.*

[2]*Consejo Nacional de Investigaciones Científicas y Técnicas (CONICET, Dpto. de Geografía y Turismo, Universidad Nacional del Sur, Argentina.*

ABSTRACT. The resolution of Digital Elevation Models (DEM) as well as the area threshold to define streams and catchments are important sources of uncertainty in automated fluvial morphometry. This study examines the applicability of three global surface models, produced with resolutions of 12.5 (ALOS), 30 and 90 m (SRTM), along with five area thresholds ranging from 0.15 to 10%. It aims at evaluating the effects of varying resolution-threshold combinations on the extraction of morphometric parameters and indices (PIm) in the Arroyo del Oro, a mountain basin located in south-western Buenos Aires (Argentina). The analysis considers the accuracy of drainage definitions, the variability of resulting PIm, and its implications for flood and water erosion assessments. Results show that the higher thresholds affect the PIm that depend on the complexity of the drainage network. Coarser resolutions impact on relief, slope and length parameters, but yield small discrepancies for the remaining PIm. For the 0.15% threshold, SRTM30 provides good fit of drainage composition parameters, and it is therefore suitable to assess the efficiency and capacity of the basin to evacuate floods. However, the use of higher resolution (ALOS12) is most suitable to assess erosion potential, due to better fit of slope-dependent PIm. Applications based on the global characteristics of middle to large-sized basins rely on a more flexible choice, as geometry parameters are unaffected by resolution and threshold.

Efectos de la resolución del DEM y de los umbrales de área en la morfometría fluvial automatizada, Arroyo del Oro (Argentina)

RESUMEN. La resolución de los Modelos Digitales de Elevación (DEM), así como el umbral de área utilizado para definir la red de drenaje, son fuentes importantes de incertidumbre en morfometría fluvial automatizada. Este estudio examina la aplicabilidad de tres modelos globales, producidos con resoluciones de 12,5 (ALOS PALSAR RTC), 30 y 90 m (SRTM), junto con cinco umbrales de área entre 0,15 y 10%. El objetivo es evaluar los efectos de las diferentes combinaciones resolución-umbral en la extracción de parámetros e índices morfométricos (PIm) en la cuenca del Arroyo del Oro, una cuenca serrana localizada en el Sudoeste Bonaerense (Argentina). El análisis considera la precisión en la definición del drenaje y los parámetros asociados, la variabilidad de los PIm resultantes y sus implicaciones para la evaluación del peligro de crecidas y erosión hídrica. Los resultados indican que los mayores umbrales afectan los PIm que dependen de la complejidad de la red de drenaje. Las resoluciones más gruesas afectan los parámetros de relieve, pendiente y longitud, pero producen pequeñas discrepancias para los PIm remanentes. El umbral de 0,15 % y la resolución de 30 m proporcionan un buen ajuste de la composición del drenaje, resultando adecuados para evaluar la eficiencia y la capacidad de la cuenca para evacuar las crecidas. Sin embargo, el uso de una resolución más alta (12,5 m) es más adecuado para evaluar el potencial de erosión, debido a un mejor ajuste de los PIm que dependen de la pendiente. Para aplicaciones basadas en las características globales

de cuencas de tamaño mediano a grande, la elección es más flexible, debido a que los parámetros de geometría no se ven afectados por resolución o umbral.

Keywords: DEM resolution, area thresholds, morphometric parameters and indices, Arroyo del Oro.

Palabras clave: resolución, umbrales de área, parámetros e índices morfométricos, arroyo del Oro.

Received: 1 September 2024

Accepted: 24 January 2025

***Corresponding author:** Ana Casado. Consejo Nacional de Investigaciones Científicas y Técnicas (CONICET), Centro de Emprendedorismo y Desarrollo Territorial Sostenible, Universidad Provincial del Sudoeste, Argentina. Email: ana.casado@uns.edu.ar

1. Introduction

The automated extraction of morphometric information from Digital Elevation Models (DEM) is a common task in fluvial assessment and modelling. While a range of hydro-processing tools are available, few studies evaluate the effectiveness of such tools or the quality of the results for morphometric assessment (Dávila Hernández *et al.*, 2022; Shekar and Mathew, 2024). There are some issues that remain to be addressed for successful extraction of morphometric information from DEMs. These are mainly linked to the DEM source and resolution, but also to the parameters used in automated hydro-processing.

The growing diversity of data sources challenges the choice of DEMs meeting optimal scale-related quality and resolution, while balancing the costs for acquisition and processing (Boulton and Stokes, 2018; Dávila Hernández *et al.*, 2022). Current trends are evolving to high-resolution terrain models obtained from photogrammetry and LiDAR techniques. However, the spatial coverage of such products is limited compared to global, space-borne elevation data, and their high cost prevents their widespread use in many countries (Boulton and Stokes, 2018; Courty *et al.*, 2019). In this context, the middle-resolution surface models derived from the Shuttle Radar Topography Mission (SRTM, NASA) have become the most globally used for hydrological modelling. Even if they contain altimetry bias due to buildings, vegetation and other elements on the terrain surface (Gallant and Read., 2016; O'Loughlin *et al.*, 2016), the popularity of SRTM DEMs relies on their free access and wide availability, along with their acceptable quality (Boulton and Stokes, 2018; Courty *et al.*, 2019; Dávila Hernández *et al.*, 2022). More recently, global surface models of higher resolution, such as ALOS PALSAR with Radiometric Terrain Correction (NASA-JAXA and ASF), among others, permitted to improve automated extraction of morphometric parameters due to their greater topographic detail (Niipele and Chen, 2019). The effects of DEM resolution on fluvial morphometry have received early attention (Hancock, 2005; Thompson *et al.*, 2001), and remain of current interest (Buakhao and Kangrang, 2016; Datta *et al.,* 2022: Nourani *et al.*, 2013; Wu *et al.*, 2017). Most studies report that the effects of resolution are not linear, as they depend on the size and the terrain complexity of the study basin. Furthermore, it has been observed that DEMs from different sources may produce greater variability than resolution for the same source. These findings highlight the diversity of sources of uncertainty in the analysis and interpretation of basin properties extracted from DEMs.

While the DEM affect the quality of the morphometric parameters being extracted, the complexity of parameters involved in runoff dynamics challenges determining the accuracy of such parameters (Shekar and Mathew, 2024). Most GIS-based hydro-processing tools available today build on the D8 algorithm (O'Callaghan and Mark, 1984), which assumes that runoff follows the direction of the terrain

gradient once it exceeds a minimum accumulation area for the conformation of a channel unit. This area threshold (*As*) constitutes the most important parameter in stream definition. In practice, *As* is defined using a standard value which is assumed as constant throughout the basin. Most GIS-based hydro-processing tools propose using 1% of maximum flow accumulation by default (Ozulu and Gökgöz, 2018). Yet a number of methods to define *As* have been early developed. These are based, among others, on stream drop and slope-area relationships (Tarboton *et al.*, 1991), on the scaling properties of stream fractal geometry (da Ros and Borga, 1997), and on variable morphologic and geologic influence within the study basin (Lopez García and Camarasa Belmonte, 1999; Montgomery and Foufoula Georgiou, 1993). Despite the value of these approaches, so far there is no global consensus on this issue (Datta *et al*., 2022; Niipele and Chen, 2019; Ozulu and Gökgöz, 2018; Wu *et al*., 2017). Moreover, the range of variability in morphometric extractions and its implications for the understanding of basin dynamics still represents an important research gap for many regions (Shekar and Mathew, 2024).

From the above, it follows that automated fluvial morphometry face two important challenges. The first is linked to the choice of an input DEM that ensures the most suitable relationship between resolution, basin size and terrain topography. The second involves the definition of an area threshold allowing for a suitable definition of the basin drainage complexity. More importantly, there are no optimal, generalized resolution-threshold combinations, as a given resolution or threshold may yield more or less suitable results depending on the context of the study and its applications in fluvial morphometry.

This paper aims at determining the effects of DEM resolution and area thresholds for automated extraction of morphometric parameters within the Arroyo del Oro (Argentina), a mountain basin that conforms the headwaters of the Sauce Grande River. It compares the applicability of popular global surface models, available with resolutions of 12.5 (ALOS), 30 and 90 m (SRTM), along with five area thresholds ranging from 0.15 to 10%. This yields fifteen possible resolution-threshold combinations. The validation of the results considers three criteria. These include the accuracy in drainage definitions and computed parameters, the variability of the resulting morphometric indices, and its implications for flood and water erosion assessment. Although the potential for transferability of the results to other regional basins remains to be evaluated, findings from this investigation provide valuable insights for making informed resolution and area threshold selection in watershed modelling, having wider testing applicability for water resources managing for a variety of spatial scales.

2. Study area

The Arroyo del Oro drains the north-eastern slopes of the Sierra de la Ventana range and flows down into the Sauce Grande River (Fig. 1). The drainage network develops over metamorphic rock in the headwaters, and excavates quaternary fluvial and wind deposits in the lower section (Gil, 2012). Headwater slopes are steep (20%, on average), while the foothills and the alluvial plain exhibit undulating to gentle topography (Volonté and Gil, 2023). Bare rock soils cover 60% of the basin. Land use is predominantly agricultural, and limited to moderately deep soils over the foothills. Except for the town of Villa Ventana, which is home to 952 people (INDEC, 2022), population density is low (0.27 hab./km^2).

The regional climate is dry subhumid (Casado, 2021). Mean annual temperature is 14.2 °C and mean annual rainfall is 725 mm (1981-2020). Rainfall variability is marked, and responds to regional circulation features (Gil *et al.*, 2008; Zapperi *et al.*, 2006; Zapperi *et al.*, 2007) as well as to global climate anomalies such as El Niño-Southern Oscillation (Scian, 2000). The stream flow regime is flashy and driven by torrential storms. Long periods of little or no flow are interspersed with floods of high relative magnitude (Casado *et al.*, 2016). Although excess water is evacuated quickly, storms and floods are frequent, and constitute a major threat to urban population and infrastructures (Gil *et al.*, 2016). In addition, soil water erosion is the main constraint to the agricultural aptitude of basin soils (INTA, 2018).

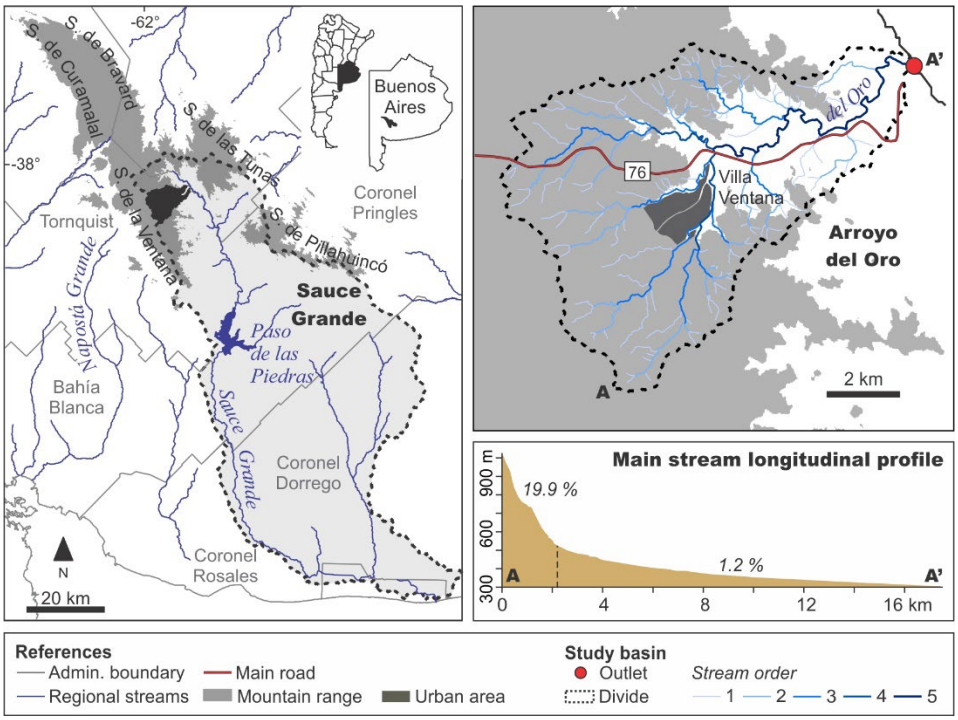

Figure 1. Map of the Arroyo del Oro basin showing main regional features.

3. Materials and methods

This study evaluates the influence of varying DEM resolution and area thresholds for automated morphometric analysis in the Arroyo del Oro basin. The analysis builds on a four-step procedure which involves (1) catchment and stream definition, (2) extraction of morphometric parameters, (3) computation of morphometric indices, and (4) validation of the results relative to the reference basin (Fig. 2).

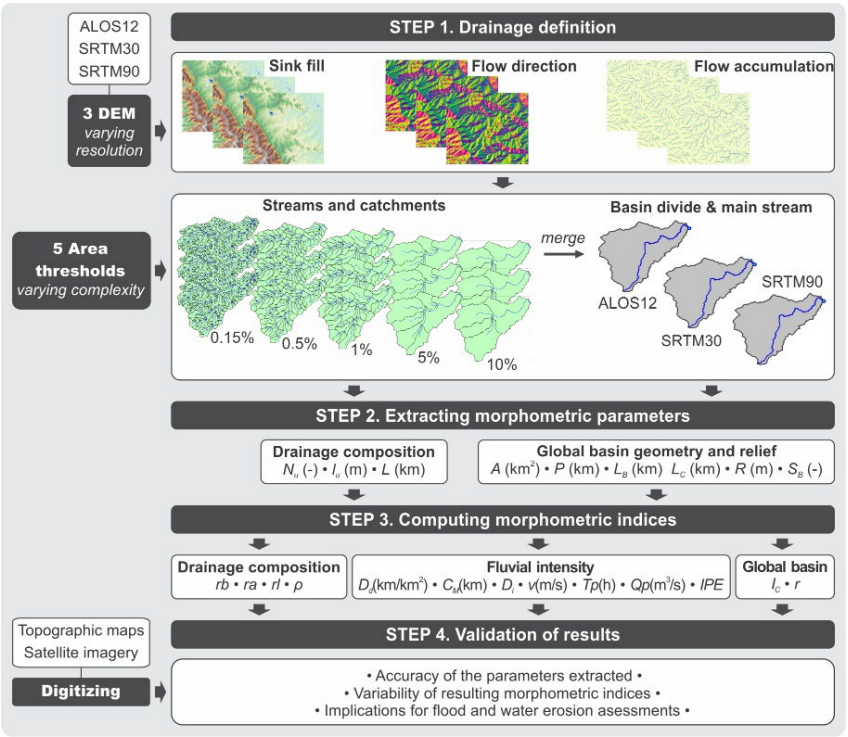

Figure 2. Methodological scheme for morphometric analysis.

3.1. DEM quality assessment

This paper uses three different DEMs with resolutions of 12.5, 30 and 90 m. All three are global surface models produced by space-borne SAR missions, SRTM (NASA) and ALOS (NASA-JAXA & ASF). Hereafter, these models are referred to as ALOS12, SRTM30 and SRTM90, respectively. Table 1 summarizes DEM metadata. Although an updated version of SRTM30 has been released in 2021 (NASADEM), it relies on an array of terrain products and auxiliary data that were not available during the original processing of SRTM (NASA JPL, 2021). The version released in 2014 (SRTMGL1) has been void filled like SRTM90, and underpin radiometric terrain correction of ALOS12. Comparatively, SRTMGL1 allows minimizing the effects of the DEM source on the resulting data, and is likely more suitable for the purpose of the study.

The ability of the models to reproduce terrain elevation and forms was evaluated in terms of accuracy and reliability. Vertical errors were determined relative to known orthometric heights, extracted from the national levelling network (RN-Ar, IGN, Argentina) for the upper Sauce Grande basin. Orthometric heights were converted to ellipsoid heights (WGS84) using two online tools, GeoidEval v2.4 (for EGM96) and GEOIDE-Ar 16 (IGN, Argentina). Errors were reported as the mean error (ME) and the root mean square error (RMSE), as indicators of bias and statistical distribution of error, respectively (Fisher and Tate 2006). Since errors are likely to vary spatially, we inspected for artefacts (padi terraces) and outliers using GIS-based neighbourhood analysis within focal windows of 3x3 cells (Hengl *et al*. 2004). Artefacts were detected using metrics of variety, where 1 indicates that all nine cells have the same elevation value, and 9 indicates the opposite. Outliers were detected using the statistical approach of Felicísimo (1994), which builds on extreme deviations of normalized residuals using a Student's *t* test. For a confidence level of 95%, the value of *t* is 1.96. The spatial offset of extracted streams relative to reference was used as a simple, additional measure of DEM reliability. Offset analysis used the longest flow path instead of the entire stream network to ensure that the results were unaffected by drainage complexity.

Table 1. Metadata of the DEMs used in the study.

Metadata	**ALOS12**	**SRTM30**	**SRTM90**
Model ID	ALPSRP240256410	SRTM1S39W062V3	SRTM3S39W062V2
Acquisition date	29/07/2010	11/02/2000	11/02/2000
Version	Radiometric Terrain Corrected (RT1) based on SRTMGL1 (05/05/2015)	SRTMGL1 - 1 Arc-Second Global Void filled (23/09/2014)	SRTMGL3 - 3 Arc-Second Global Void Filled (17/04/2013)
Projection	WGS84 UTM20S	WGS84	
Horizontal datum	WGS84		
Vertical datum	Earth Gravitational Model 1996 (EGM96)		
Height	Ellipsoid (WGS 84)	Geoid (EGM96)	Geoid (EGM96)
Spatial resolution	12.5 m	1 arc-second (~30 meters)	3 arc-seconds (~90 meters)
Raster size	~0.5º lat / ~1º lon	1 degree tiles	1 degree tiles
Centre coord.	-38.0 / -62.1	-38.5 / -61.5	

3.2. Drainage definition

Streams and catchments were defined from each DEM using HEC-HMS GIS module (v4.11, U.S. Army Corps of Engineers). For each model, we computed flow direction and flow accumulation layers using standard sink and drainage pre-processing parameters (Fig. 2). This yielded three sets of drainage data from which to define the streams and their catchments.

In practice, the minimum drainage area to define a stream is 1% of the basin surface (USACE, 2023). This is the default for most GIS-based hydro-processing tools (Ozulu and Gökgöz, 2018), and

thus represents a standard area threshold. However, the lower (or higher) the area threshold (*As*), the greater (or smaller) the complexity of the stream network being extracted. Even though many morphometric parameters depend on the drainage complexity, some others do not. Thus, a given *As* may be more or less suitable relative to varying applications in fluvial morphometry. Moreover, the lower the *As*, the greater the processing requirements relative to the basin size. In this regard, *As* should also provide a reasonable balance between topographic detail and processing capacities for a given study basin. In this paper, we tested four additional area thresholds below and above the standard 1% (Table 2). These take arbitrary values of 0.15%, a low threshold involving reasonable processing times, and of 10%, a high threshold allowing detecting a bound depicting main streams and catchments; the values of 0.5 and 5% were used to inspect for potential intermediate breaks.

The combination of three DEMs and five area thresholds yielded fifteen sets of drainage elements. All layers were exported to a Geographical Information System (GIS). Area, length, and other basic statistics were obtained from the attribute tables.

Table 2. Contributing area thresholds used in the study and number of equivalent grid cells by DEM.

A_s (%)	Area (km^2)	Grid cell number		
		ALOS12	SRTM30	SRTM90
0.15	0.1	595	121	13
0.5	0.3	1984	404	45
1	0.6	3968	809	90
5	3.1	19840	4043	449
10	6.2	39680	8086	898

3.3. Morphometric parameters and indices

We considered a range of morphometric parameters and indices (PIm) popularly used for flood and water erosion assessments (Table 3). Following Romero Díaz and López Bermúdez (1987), parameters are different from indices in that the latter result from a relationship between two or more parameters. To ensure the readability of the results, PIm were assembled into three groups. These account for (i) global basin characteristics, (ii) drainage composition, and (iii) a set of indices designating the intensity of fluvial processes.

Table 3. Morphometric parameters and indices used in the study.

(i) Global basin characteristics: geometry and relief

PIm	**Equation**	**Application**	**Reference**
Area	A (km^2)	Input parameter for basin shape and fluvial intensity indices	-
Perimeter	P (km)	Input parameter for basin shape indices	-
Basin length	L_B (km)	Input parameter for basin shape indices	
Longest flow path	L_C	Input parameter for velocity and flood hydrograph parameters: Qp & Tp	
Mean basin slope	S_B (%)	Input parameter for velocity and erosion potential indices	
Basin relief	$R(\mathrm{m}) = \max\Delta Z$ (1)	Maximum gradient of the basin	Schumm (1956)
Relief ratio	$r = R/L_B$ (2)	Indicates the geomorphic evolution of basins	Schumm (1956)
Compactness coefficient	$m = 0.282P/\sqrt{A}$ (3)	Basin shape index designating both the intensity and erosive capacity of floods	Gravelius (1914)

(ii) Drainage composition

PIHm	Equation	Description	Reference
Stream number	N_u	Input parameter for drainage composition and fluvial intensity indices.	Horton (1945)
Average stream length	l_u (km)	Input parameter for drainage composition and fluvial intensity indices	Horton (1945)
Total length	L (km)	Input parameter for drainage density index	Horton (1945)
Bifurcation ratio	$rb = N_u/N_{u+1}$ (4)	Indicates how water flows and branches within a basin (drainage composition)	Horton (1945)
Length ratio	$rl = l_u/l_{u-1}$ (5)	Indicates the hierarchical structure and connectivity of stream networks within a basin (drainage development)	Horton (1945)
Rho coefficient	$\rho = rl/rb$ (6)	Indicates channel storage capacity to evacuate floods.	Horton (1945)

(iii) Fluvial intensity

PIHm	Equation	Description	Reference
Drainage density	$D_d(\mathrm{km/km^2}) = L/A$ (7)	Measures the stream distribution by basin area. High drainage density indicates higher and faster floods	Horton (1945)
Constant of channel maintenance	$C_M(\mathrm{km}) = 1/D_d$ (8)	The inverse of Dd indicates sediment transport capacity and erosion potential of drainage networks	Schumm (1956)
Drainage intensity	$D_i = D_d(N_1/A)$ (9)	Indicates both efficiency and capacity of drainage networks to evacuate torrential rainfall	Romero Díaz and López Bermúdez (1987)
Flow velocity	$v(\mathrm{m/s}) = 0.278(L_C/T_c)$ (10)	Input parameter for Qp and Tp (T_c computed with CN = 73)	NRCS (2010)
Peak discharge	$Qp(\mathrm{m^3/s}) = 0.278A\ qp$ $qp = (1.31/L_C)rl^{0.43}v$ (11)	Maximum instantaneous discharge during a high-rainfall event (dynamics of flood events)	Rodríguez Iturbe and Valdés (1979)
Time to peak	$Tp(\mathrm{h}) = \frac{0.44L_C rb^{0.55} ra^{-0.55} rl^{-0.38}}{v}$ (12)	Time interval between the beginning of effective rainfall and the peak discharge (dynamics of flood events)	Rodríguez Iturbe and Valdés (1979)
Potential erosion index	$IPE = (D_i S_B)/m$ (13)	Integrates the three erosion enhancing factors: drainage intensity, average slope and shape	Ferrando (1994)

3.4. Validation of results

The quality of the results obtained for each resolution-threshold combination was determined relative to the basin of reference (Fig. 2). Validation involved inspecting for the accuracy in drainage definitions and computed parameters, the variability of resulting morphometric indices, and the implications for flood and water erosion assessments. The stream network was digitized from an Ikonos satellite image captured in 2003 (Google Earth historical archive; © 2022 Maxar Technologies). In addition to exhibiting good quality and resolution, the year of capture falls within the radar missions from which the MDE were derived (2000 and 2010). This permitted to reduce potential shifts resulting from the natural evolution of vegetation and landforms. The basin divide was digitized from a topographic map following the inflections of contour lines (3763-36-3, 1:50,000; IGN, Argentina). The map was projected using the spatial reference transformations defined by the IGN (Campo Inschauspe to POSGAR94, and POSGAR94 to WGS84) to ensure the spatial integrity of the analysis. Relief parameters were also obtained from the topographic map. In this case, however, vertical adjustment was considered unnecessary because basin relief and slope depend on relative elevation differences. Reference PIm were computed from attribute tables and 3D analysis in GIS.

4. Results and discussion

4.1. DEM accuracy and reliability

Known elevations available from the RN-Ar levelling network range from 199 to 441 m (23 points). Coefficients of determination of equivalent DEM elevation values were close to unity for all three models (0.99), suggesting a very good fit (Fig. 3). Mean errors increased with lower resolution from 3.9 to 4.1 m; this was between 1.4 and 1.5% of known elevations. The error dispersion (RMSE) increased with lower resolution as well from 7.6 to 8.1 m. Accuracy loss with lowering resolution is closely related to complex terrain (Fisher and Tate, 2006), and results from a systematic attenuation of the relief as the DEM resolution becomes coarser (Buakhao and Kangrang, 2016; Datta *et al*., 2022). Major errors were between 11 and 25ºm, and responded mainly to vegetation bias irrespective of resolution. Certainly, SRTM and ALOS DEMs are surface models, and therefore contain vertical noise due to buildings, vegetation and other elements on the terrain surface (Gallant and Read, 2016; Nourani *et al*., 2013; O'Loughlin *et al*., 2016).

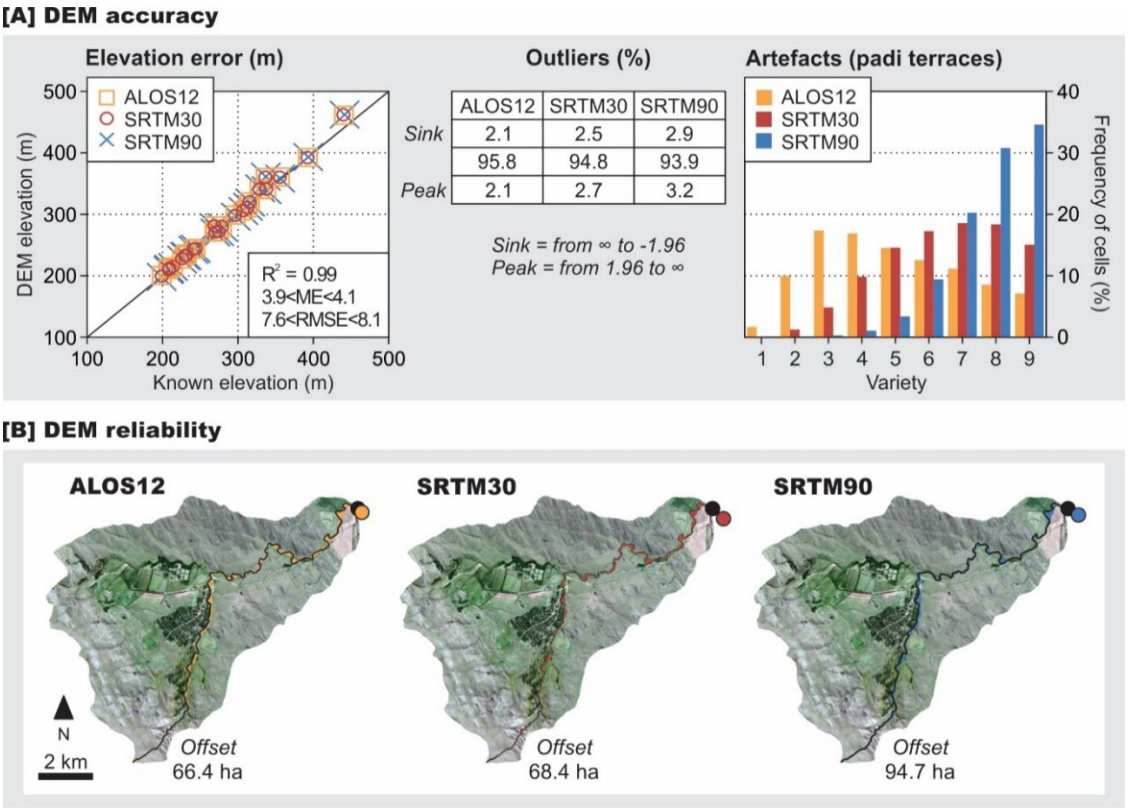

Figure 3. Quality of the input DEMs.

Relative error assessment suggested acceptable DEM quality as well. Outliers were between 4.2 and 6.1%, and at least one cell value was different from the remaining eight neighbouring cell values for 98% of the study basin or more (Fig. 3). Interestingly, the frequency of cells for increasing levels of elevation variety describes contrasting distributions among DEMs. While ALOS12 exhibits a right-skewed distribution (greater proportion of artefacts), SRTM30 distribution is skewed to the left (lesser proportion of artefacts), and SRTM90 is exponentially artefact-free. This responds to the artefact dependence on the spatial and vertical resolution of the source data relative to the terrain forms (Hengl *et al*., 2004). All three DEMs are integer rasters. This implies that any elevation difference between adjacent grid cells is at least 1 m, and corresponding slopes are 1% (SRTM90), 3% (SRTM30), and 8% (ALOS12). In this regard, artefacts are expected to increase with increasing resolution along with flat terrain.

The spatial offset of DEM-extracted main streams relative to reference was less than 1.5% of the basin surface, suggesting that all three models are reliable to reproduce flow patterns (Fig. 3). However, some stream sections revealed important shifts. This responds to complex relationships between resolution and topography (Buakhao and Kangrang, 2016; Thompson *et al*, 2001; Wu *et al*., 2008), along with morphological variations for the same resolution (Boulton and Stokes, 2018), and vegetation noise (Nourani *et al*., 2013). In the upper basin (S_B = 40%), the fluvial network integrates a branch of v-shaped streams excavated on bedrock with little or no vegetation (Volonté and Gil, 2023). Here, the algorithm is not affected by aggregated elevation values nor vegetation inducing false reliefs, and stream definitions are acceptable for all three models. In the middle and lower sections (S_B = 14%), the main stream excavates quaternary deposits forming a wider channel. The influence of resolution is here apparent yet not widespread, and depends on both stream morphology and vegetation cover. In sections lacking riparian vegetation, lower resolution DEMs smooth channel landforms, and therefore fail to define streams in dynamic sections. This was observed for SRTM90 throughout the entire stream. On the other hand, vegetation bias results in false positive reliefs that shift the stream towards adjacent, lower terrain. In these cases, the higher the resolution, the greater the noise and the greater the probability of computing vegetation as a topographic feature. At the basin scale, however, the advantages (topographic detail) and disadvantages (noise) of higher resolution compensate and, in terms of shift, the quality of the streams extracted from SRTM30 and ALOS12 is higher than that extracted from SRTM90.

4.2. Global basin morphometric parameters

Global basin parameters are affected by DEM resolution only. Basin area and length fit well to reference for all three DEMs (Fig. 4). Notable differences are found for the basin perimeter though, with overestimations ranging from 34% (SRTM90) to 47% (ALOS12) of the reference value. This behaviour may obey to the gridded structure of the models (Wu *et al.*, 2008). Since *P* represents the sum of the sides of the grid cells along the basin divide, the greater the number of cells with increasing resolution, the larger the resulting length. We computed a correction factor (FC) to account for the number of cells along the divide for a given resolution (p). The expression to obtain a corrected value of *P* is as follows: $P_C = [P / (FC\ p)]\ (p\ 2^{0.5})$. Given FC≈2, the P_C was 36.6 (SRTM90), 36.8 (SRTM30) and 37.0 (ALOS12). Hereafter, any PIm involving the basin perimeter will use P_C values instead of original *P*.

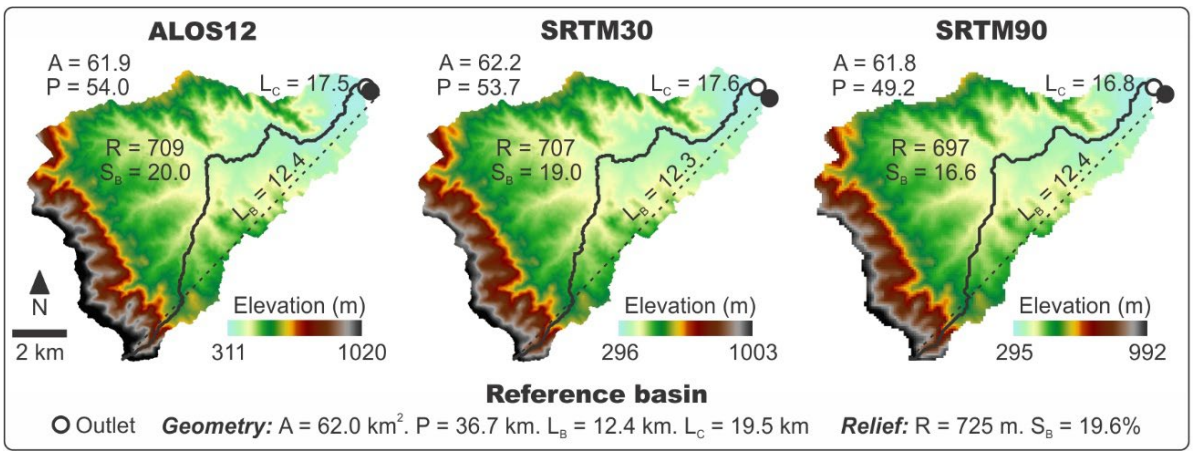

Figure 4. Global basin morphometric parameters for the Arroyo del Oro by DEM resolution.

The effects of the gridded structure of DEMs impact on the longest flow path length as well (L_C; Fig. 4). However, in opposition to *P*, L_C is underestimated in all cases, and remains up to 2 km below the reference length for the best fit (ALOS12). This is a consequence of the way streams are defined. As the algorithm links cell centroids in the flow direction (Wu *et al.*, 2008), one may expect that the

larger the cell size, the larger the length. However, if the channel width is close to (or less than) the grid cell size, then the streams will be defined by straight lines irrespective of their sinuosity, which ultimately affects their total length (Boulton and Stokes, 2018). The ratio of L_C to L_B (Schumm, 1956) represents a straightforward index to determine whether the reduced length is due to the DEM structure, to the DEM resolution, or to a combination of both. For the Arroyo del Oro, this ratio ranges from 1.36 (SRTM90) to 1.43 (ALOS12), remaining between 14 and 10% below reference, respectively. Considering that L_B fits very well for all three models, this suggests that even the smaller cell size used in analysis (12.5 m) is insufficient to capture the sinuosity of the main stream channel.

The effects of DEM resolution are more evident when global relief parameters are considered (Fig. 4). The greater the grid cell size, the greater the terrain smoothing (Buakhao and Kangrang, 2016; Wu *et al.*, 2017), and so the basin relief and slope decrease along with decreasing resolution. In addition, the literature reports that terrain smoothing is greater for steep slopes than for flat reliefs. This is of particular interest within mountain basins, where steep and rolling lands dominate over flatlands. For the Arroyo del Oro, the average basin slope was affected by resolution up to 15% below reference (SRTM90), remaining 2% below reference for the model of highest resolution (ALOS12).

4.3. Parameters of drainage composition

Automated stream definition typically differs from reference drainage networks (Niipele and Chen, 2019). In some cases, this is due to scale issues concerning the document used as a base for reference (Gil *et al.*, 2019). On most cases, however, this results from inadequate estimations of the minimum area required to define a stream. Figure 5 illustrates the effects of varying area thresholds (*As*) along with varying DEM resolution for stream definition in the Arroyo del Oro basin. Since higher thresholds imply higher minimum areas for a stream channel to initiate (O'Callaghan and Mark, 1984), the larger the area threshold, the greater the impact on the definition of first-order streams. Increasing thresholds result into a progressive simplification of the drainage complexity, and consequently impact on the indices involving Horton's ratios. The best fit was found for the smaller threshold for all parameters and across all three models (Fig. 5).

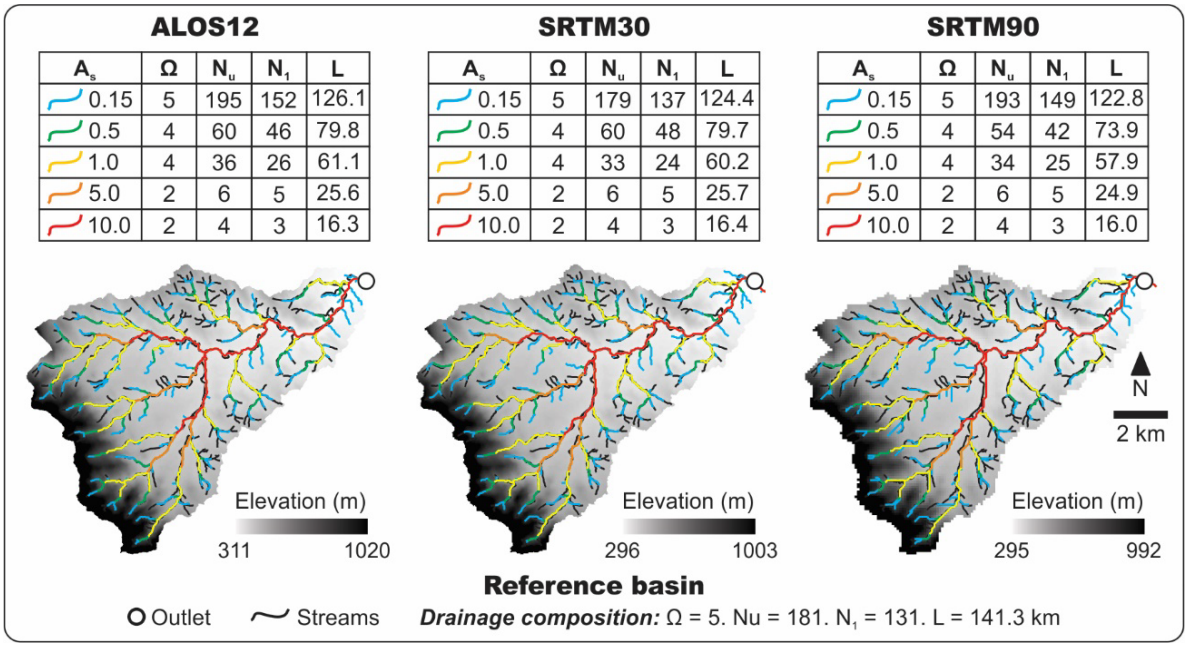

A_s	Ω	N_u	N_1	L
0.15	5	195	152	126.1
0.5	4	60	46	79.8
1.0	4	36	26	61.1
5.0	2	6	5	25.6
10.0	2	4	3	16.3

A_s	Ω	N_u	N_1	L
0.15	5	179	137	124.4
0.5	4	60	48	79.7
1.0	4	33	24	60.2
5.0	2	6	5	25.7
10.0	2	4	3	16.4

A_s	Ω	N_u	N_1	L
0.15	5	193	149	122.8
0.5	4	54	42	73.9
1.0	4	34	25	57.9
5.0	2	6	5	24.9
10.0	2	4	3	16.0

Figure 5. Drainage composition of the Arroyo del Oro by area threshold and DEM resolution.

The effects of resolution on drainage composition are more apparent for the stream length than for the number of streams (Fig. 5). While *L* increases with resolution like L_C, N_u and N_1 vary among the models with unclear relationships. Visual comparison to reference shows that all DEMs provide fairly accurate delineations of higher order streams, but not accurate enough for the lowest orders. Major shifts concern first-order streams. Many collectors in the headwaters are omitted, whereas many false segments are depicted along the main streams. However, omissions and additions compensate for the entire basin, with SRTM30 providing the best fit. Similar results were found by Li and Wong (2010), who suggested that an optimal threshold may not exist for the entire basin due to local variations in topography. This was reported by early studies (Lopez García and Camarasa Belmonte, 1999; Montgomery and Foufoula Georgiou, 1993), by Lee and Kim (2011), and more recently by Wu *et al*. (2017). Another possible source for this problem was more recently proposed by Dávila Hernández *et al.* (2022), who found that fill sink and flow routing algorithms, relative to the DEM resolution, may affect the definition of pits governing the water movement through the model. Similarly, Wang *et al*. (2019) reviewed existing sink-processing algorithms, and discussed existing ways of improving their computation efficiency to provide a satisfactory solution to this issue.

4.4. Morphometric indices

Table 4 summarizes the indices that depend on global characteristics of the drainage basin, and so are unaffected by the area threshold. The compactness coefficient (*m*) is within the limits of variation for slightly rectangular basins (Zavoianu, 1985), with very good fit and small differences among the three models. This occurs because basin area and perimeter (corrected) adjust well for all DEMs, and are therefore suitable for basin shape-derived indices. The relief ratio exhibits good fit as well, and therefore indicates that terrain smoothing with increasing grid cell size has no major implications relative to the basin length. The effects of DEM resolution emerge for flow velocity, and respond to both reduced L_C and S_B for all models, with maximum difference for SRTM90.

Table 4. Basin geometry- and relief-derived morphometric indices for the Arroyo del Oro by DEM resolution.

Morphometric Index	Reference basin	ALOS12	SRTM30	SRTM90	Best fit (%)	Max. difference (%)
Compactness coeff. (m)	1.31	1.31	1.31	1.31	--	--
Relief ratio (r)	0.06	0.06	0.06	0.06	--	--
Flow velocity (v, m/s)	4.43	4.36	4.28	4.02	-1.7 (ALOS12)	-9.3 (SRTM90)

The remaining indices depend on the drainage composition to a greater or lesser extent, and are therefore affected by both DEM resolution and area threshold. Errors in index estimations were computed as residuals between extracted and reference PIm for each resolution-threshold combination. To ensure readability of the results, errors are expressed as deviations relative to reference values (Fig. 6). Since the best fit for drainage parameters was found for the lowest area threshold, all indices exhibit the smaller deviations for $As = 0.15\%$. In terms of resolution, however, no generalizations can be made through the indices. This is due to compensation and/or accumulation of errors resulting from computation of the parameters involved in each case. Resolution-related deviations behave differently among the indices, and will have different implications for flood and water erosion assessment.

Bifurcation and length ratios (*rb*, *rl*) provide information on the basin efficiency and capacity to evacuate flows (Zavoianu, 1985), and remain of current interest for flood assessment (Shekar and Mathew, 2024). For $As = 0.15\%$, *rb* and *rl* exhibit good fit for the three models (Fig. 5), and remain within the normal range for mountain basins with good drainage capacity (Horton, 1945). Deviations of the bifurcation ratio are positive and greater in magnitude than for the length ratio. This is due to overestimation of first-order streams, and concerns the three DEMS. Shorter stream lengths, as provided

by all models, do not necessarily affect *rl* because such reduction remains constant among orders. Thus, *rl* deviations remain below 2% of the reference value, and compensate the deviations of *rb* for computation of the rho coefficient. Note that the perfect fit of ρ for *As* = 1% is specious, and results from *rb* and *rl* deviations of similar magnitude and direction. For *As* > 1%, *rb* and *rl* deviations result in values of ρ greater than 82% of reference values, denoting drainage basins with greater attenuation of flows and erosion (Horton, 1945).

The peak discharge (*Qp*) and the time to peak (*Tp*) are the basic parameters of the direct runoff hydrograph. In this study, *Qp* and *Tp* were computed based on the Geomorphological Instantaneous Unit Hydrograph (GIUH) developed by Rodríguez Iturbe and Valdés (1979), which links the unit hydrograph with Horton's laws. The best fit for *Qp* is found for area thresholds below the standard (Fig. 5), with deviations between 3% (SRTM90) and 8% (ALOS12) for *As* = 0.15%. Considering that *Qp* is a product of velocity, and that velocity is underestimated for the three resolutions (Table 4), it follows that positive deviations of *Qp* respond to lower drainage capacity due to shorter main stream length, L_C. This ultimately leads to greater water accumulation, and so *Qp* values are higher than reference. The time to peak exhibited very good fit for the three DEMs, with differences between 1% (ALOS12) and 9% (SRTM90). Here, shorter L_C values compensate with higher *rb*, while *rl* values remain close to reference in all three cases. The best fit is obtained for ALOS12, as it yields the smallest deviations for the majority of the PIm involved in computation of both *Qp* and *Tp*.

Deviations of the remaining indices are linked to the area threshold more than to the DEM resolution (Fig. 6). Increasing *As* leads to reduced total length, with deviations up to -89% (SRTM90) for the highest threshold (*As* = 10%). This consequently affects drainage density (D_d) and the constant for channel maintenance (C_M). Best fits are found for *As* = 0.15%, although shorter stream lengths lead to D_d deviations between -11% (ALOS12) and -13% (SRTM90) relative to the reference basin. Because all three models provide a greater number of first-order streams, N_1 compensates for reduced total length, and the drainage intensity D_i shows better fit than the drainage density. Yet D_i deviations increase notably with increasing thresholds due to progressive simplification of the stream network, and have greatest influence on the erosion potential index.

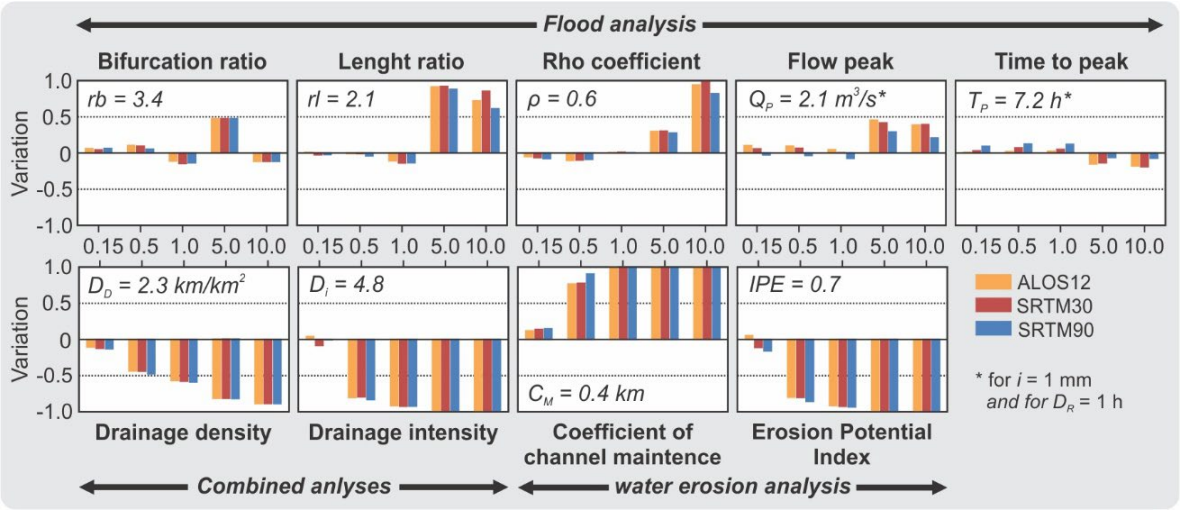

Figure 6. Deviation of morphometric indices relative to reference values by DEM resolution and area threshold. Arroyo del Oro basin.

4.5. What resolution and what threshold for what application?

The accuracy of global basin parameters will depend primarily on the choice of the input DEM, as these properties do not depend on the definition of streams. Within the Arroyo del Oro basin, all three DEMs yielded acceptable results for area, perimeter (corrected), basin length, and shape-related indices (Fig. 7). This is an interesting outcome, suggesting that studies based on applications other than terrain description may rely on middle- to low-resolution DEMs without significant performance loss. On the other hand, slope was clearly affected by resolution, with the best fit for ALOS12. Yet SRTM models yielded acceptable results as well, and thus may provide important processing benefits in cases where the basin size represents a computational challenge (Boulton and Stokes, 2018; Buakhao and Kangrang, 2016; Courty *et al*., 2019). In addition, results showed that area thresholds greater than standard may notably contribute to reduce the number of basins units to merge for global geometry and relief analysis. While the 10% threshold (6.2 km^2) allowed detecting the main subbasins identified for the study area, trial and error analysis revealed that thresholds of 25% (15.5 km^2) or greater may be used to obtain a single basin unit along with its corresponding longest flow path, which ultimately allows avoiding subbasin merging.

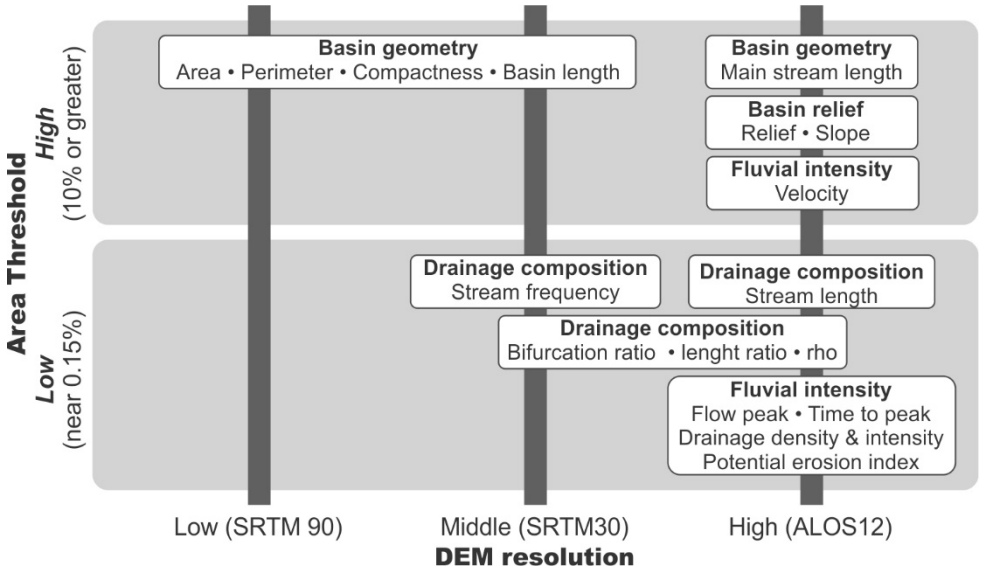

Figure 7. Synthesis of the results.

PIm relying on the accuracy of the drainage network exhibited strong dependence on the area threshold, with 0.15% providing the best results (Fig. 7). Trial and error revealed that thresholds greater than 0.1 km^2 (~0.17%) resulted on stream frequency and length reductions of up to 6 and 15%, respectively, affecting all composition and intensity indices. Results for thresholds below 0.09 km^2 (~0.14%) showed improvements of the stream length, but overestimation of the stream frequency. This resulted in better adjustment of drainage density and *Dd*-derived indices, but yielded greater shifts for the indices depending on the number of streams. Accordingly, the best match is near 0.1 km^2, and it is therefore close to the threshold tested here. Even though the potential for transferability of such threshold to other regional basins remains to be evaluated, these results highlight the potential risks of the systematic use of most popular hydro-processing tools. Indeed, the 1% threshold resulted in the omission of first-order streams by 82%, and reduced the total stream length by 57%.

The relationship between accuracy and resolution for the same threshold was comparatively less clear, due to the compensation (or accumulation) of errors in the extraction of morphometric parameters. For drainage composition PIm, resolution-related differences were not much important and, for *As* = 0.15%, results were within the range of variability of the reference basin. Comparatively, SRTM30

yielded the best balance between accuracy and processing demand, being particularly suitable for flood-related studies building on Horton ratios, while ALOS12 provided better slope and length adjustment, being best suited to flood and water erosion applications using indices of fluvial intensity.

4.6. Further research perspectives

Regardless of the acceptable quality of the results, we identified some issues in the definition of the streams that merit further investigation. First, all three DEMs failed to define first-order streams, omitting collectors in the headwaters and depicting false segments in the middle and lower sections. This may be related to the effects of local topography and geology on the definition of an optimal area threshold for the entire basin (Lee and Kim, 2011; Li and Wong, 2010; Wu *et al*., 2017), as well as to the use of standard algorithms for fill sink and flow routing (Dávila Hernández *et al.*, 2022; Wang *et al*., 2019), depicting two important issues that need to be addressed before extracting topographic attributes and terrain features from DEMs. Second, input DEMs used in this study are global surface models, and therefore contain vegetation bias that result in greater noise as the model resolution becomes finer (Nourani *et al*., 2013). In this regard, further research should evaluate the potential accuracy benefits of using bare-earth models (Gallant and Read, 2016; O'Loughlin *et al*., 2016), as well as the newer version of the SRTM30 (NASADEM), offering updated and refined elevation data. Furthermore, elevation data used in the study is 24 year-old (SRTM) and 14 year-old (ALOS). Thus, exploring for evolving links between fluvial forms and processes along with land use change, by means of automated morphometry, would strengthen the temporal validity of the results. Although these approaches exceed the scope of the present study, they inform of the complexity of parameters involved in extracting reliable drainage networks from DEMs. Therefore, they open to an array of further research perspectives that need to be addressed prior to evaluating the potential of transferability of the present results to other regional basins.

5. Conclusions

Automated morphometric analysis deals with two important challenges. These are linked to the choice of a suitable DEM resolution, and to the definition of an area threshold that holds for reference Horton's ratios. This study examined and compared the applicability of three global DEMs of different resolution (ALOS12, SRTM30 and SRTM90 m) and five area thresholds (0.15 to 10%) for the extraction of morphometric parameters and indices (PIm) within a mountain basin with varying topography. The results indicated that neither optimal nor generalized resolution-threshold combinations may be derived among PIm. In applications that depend on drainage composition, the definition of an appropriate threshold is more important than the resolution of the input model. The best fit was found for As = 0.15% for all three DEMs, with differences that remained within the range of variability of the reference basin in all cases. Comparatively, SRTM30 provided the best balance between accuracy and time processing, being particularly suitable for applications linked to flood assessment. In the case of studies focusing on the erosion potential of basins, however, ALOS12 may yield better results as it fits better for slope-dependent parameters and indices. In the context of applications based on global basin parameters, the use of lower resolution and higher area thresholds may contribute to reduce processing times without significant performance loss. Despite the analysis focused on a 62 km^2 pilot basin, findings from this investigation inform on the regular issues linked to data and parameter selection decisions in watershed modelling, having wider testing applicability to other regional basins along with varying spatial scales.

Acknowledgements

The authors dully thank the international space agencies, the National Aeronautics and Space Administration of the USA (NASA) and the Japan Aerospace Exploration Agency (JAXA), as well as the Alaska Satellite Facility (ASF) and the Instituto Georgáfico Nacional (IGN Argentina) for providing

open access to terrain data. Funding was provided by the National Council of Scientific and Technical Research (CONICET) through the Multi-year Research Project (PIP, for its Spanish acronym) with code number 2022/24 0358, and by the Secretaría de Ciencia y Tecnología de la Universidad Nacional del Sur through the Research Group Project (PGI, for its Spanish acronym) with code number 24/G092.

References

Boulton, S.J., Stokes, M., 2018. Which DEM is best for analyzing fluvial landscape development in mountainous terrains? *Geomorphology* 310, 168-187. https://doi.org/10.1016/j.geomorph.2018.03.002

Buakhao, W., Kangrang, A., 2016. DEM resolution impact on the estimation of the physical characteristics of watersheds by using SWAT. *Advances in Civil Engineering* 2016, e8180158. https://doi.org/10.1155/2016/8180158

Casado, A., 2021. Rainfall-runoff modelling in dryland catchments, Sauce Grande, Argentina. *Tecnología y ciencias del agua* 12, 254-303. https://doi.org/10.24850/j-tyca-2021-05-06

Casado, A., Peiry, J.-L., Campo, A.M., 2016. Geomorphic and vegetation changes in a meandering dryland river regulated by a large dam, Sauce Grande River, Argentina. *Geomorphology* 268, 21-34. https://doi.org/10.1016/j.geomorph.2016.05.036

Courty, L.G., Soriano Monzalvo, J.C., Pedrozo Acuña, A., 2019. Evaluation of open-access global digital elevation models (AW3D30, SRTM, and ASTER) for flood modelling purposes. *Journal of Flood Risk Management* 12, e12550. https://doi.org/10.1111/jfr3.12550

da Ros, D., Borga, M,. 1997. Use of digital elevation model data for the derivation of the geomorphological instantaneous unit hydrograph. *Hydrological processes* 11, 13-33. https://doi.org/10.1002/(SICI)1099-1085(199701)11

Dávila Hernández, S., González Trinidad, J., Júnez Ferreira, H.E., Bautista Capetillo, C.F., Morales de Ávila, H., Cázares Escareño, J., Ortiz Letechipia, J., Robles Rovelo, C.O., López Baltazar, E.A., 2022. Effects of the Digital Elevation Model and hydrological processing algorithms on the geomorphological parameterization. *Water* 14, 2363. https://doi.org/10.3390/w14152363

Datta, S., Karmakar, S., Mezbahuddin, S., Hossain, M.M., Chaudhary, B.S., Hoque, M.E., Abdullah Al Mamun, M.M., Baul, T.K., 2022. The limits of watershed delineation: implications of different DEMs, DEM resolutions, and area threshold values. *Hydrology Research* 53, 1047-1062. https://doi.org/10.2166/nh.2022.126

Felicísimo, A.M., 1994. Parametric statistical method for error detection in digital elevation models. ISPRS *Journal of Photogrammetry and Remote Sensing* 49, 29-33. https://doi.org/10.1016/0924-2716(94)90044-2

Ferrando, F.J., 1994. Métodos hidromorfométricos para determinar la erosividad en cuencas hidrográficas. *Tecnología y ciencias del agua* 9, 5-14.

Fisher, P.F., Tate, N.J., 2006. Causes and consequences of error in digital elevation models. *Progress in Physical Geography* 30, 467-489. https://doi.org/10.1191/0309133306pp492ra

Gallant, J., Read, A., 2016. A near-global bare-Earth DEM from SRTM. The International Archives of the Photogrammetry, *Remote Sensing and Spatial Information Sciences* 41, 137-141. https://doi.org/10.5194/isprs-archives-XLI-B4-137-2016

Gil, V., 2012. Geomorfología y procesos de vertiente. Cuenca alta del río Sauce Grande (Buenos Aires, Argentina). *Cuaternario y Geomorfología* 26, 133-150.

Gil, V., Gentili, J., Campo, A.M., Jelinski, G., Crisafulli, M., 2016. Evaluación del peligro potencial de crecidas en cuencas serranas. Sistema de Ventania, provincia de Buenos Aires. *III Encuentro de Investigadores en Formación en Recursos Hídricos,* Ezeiza, Argentina.

Gil, V., Volonte, A., Campo, A.M., 2019. Índices morfométricos a diferentes escalas aplicados al peligro de crecidas en cuencas pequeñas. Cuenca del arroyo San Bernardo, Argentina. *Revista Brasileira de Geomorfologia* 20, 811-824. https://dx.doi.org/10.20502/www.ugb.org.br

Gil, V., Zapperi, P., Campo, A.M., Iuorno, M.V., Ramborger, M.A., 2008. Análisis de las precipitaciones de otoño y primavera en el Suroeste bonaerense. *VII Jornadas de Geografía Física,* Jujuy, Argentina.

Gravelius, H., 1914. *Grundriß der gesamten Gewässerkunde. Band I: Flußkunde (Compendium of Hydrology. Volume I: Rivers)*. Göschen, Berlin, Germany.

Hancock, G.R., 2005. The use of digital elevation models in the identification and characterization of catchments over different grid scales. *Hydrological Processes* 19, 1727-1749. https://doi.org/10.1002/hyp.5632

Hengl, T., Gruber, S., Shrestha, D., 2004. Reduction of errors in digital terrain parameters used in soil-landscape modelling. *International Journal of Applied Earth Observation* 5, 97-112. https://doi.org/10.1016/j.jag.2004.01.006

Horton, R.E., 1945. Erosional development of streams and their drainage basins: hydrophysical approach to quantitative morphology. *Bulletin of the Geological Society of America* 56, 275-370.

INDEC, 2022. Censo Nacional de Población, Hogares y Viviendas 2022. Bases de datos REDATAM. Available at: https://redatam.indec.gob.ar/ (last access: 23/12/2024).

INTA, 2018. Carta de suelos de la República Argentina. 3963-5 TORNQUIST Available at: https://zenodo.org/records/7837681 (last access: 23/12/2024).

Lee, G., Kim, J.C., 2011. Comparative analysis of geomorphologic characteristics of DEM-based drainage networks. *Journal of Hydrologic Engineering* 16, 137-147. https://doi.org/10.1061/(ASCE)HE.1943-5584.0000295

Li, J., Wong, D., 2010. Effects of DEM sources on hydrologic applications. *Computers, Environment and Urban Systems* 34, 251-261. https://doi.org/10.1016/j.compenvurbsys.2009.11.002

Lopez García, M.J., Camarasa Belmonte, A.M., 1999. Use of geomorphological units to improve drainage network extraction from a DEM: Comparison between automated extraction and photointerpretation methods in the Carraixet catchment (Valencia, Spain). *International Journal of Applied Earth Observation and Geoinformation* 1, 187-195. https://doi.org/10.1016/S0303-2434(99)85012-0

Montgomery, D.R., Foufoula Georgiou, E., 1993. Channel network source representation using digital elevation models. *Water Resources Research* 29, 3925-3934. https://doi.org/10.1029/93WR02463

NASA JPL., 2021. *NASADEM Merged DEM Global 1 arc second V001*. Distributed by OpenTopography. https://doi.org/10.5069/G93T9FD9. Accessed: 2024-12-16

Niipele, J.N., Chen, J., 2019. The usefulness of alos-palsar dem data for drainage extraction in semi-arid environments in The Iishana sub-basin. *Journal of Hydrology: Regional Studies* 21, 57-67. https://doi.org/10.1016/j.ejrh.2018.11.003

Nourani, V., Mokhtarian-Asl, S., Khosravi-Sorkhkolaee, M., Sharghi, E., 2013. Effect of DEM type and resolution in extraction of hydro-geomorphologic parameters. In: V. Mladenov (Ed.), *Recent Advances in Continuum Mechanics, Hydrology and Ecology*. WSEAS, Rhodes Island, Greece, pp. 98-103.

NRCS, 2010, *Part 630: Hydrology, Chapter 15: Time of concentration*. Natural Resources Conservation Service, USDA, Washington DC, USA, 29 pp.

O'Callaghan, J.F., Mark, D.M., 1984. The extraction of drainage networks from digital elevation data. *Computer vision, graphics, and image processing* 28, 323-344. https://doi.org/10.1016/S0734-189X(84)80011-0

O'Loughlin, F.E., Paiva, R.C., Durand, M., Alsdorf, D., Bates, P., 2016. A multi-sensor approach towards a global vegetation corrected SRTM DEM product. *Remote Sensing of Environment* 182, 49-59. https://doi.org/10.1016/j.rse.2016.04.018

Ozulu, I.M., Gökgöz, T., 2018. Examining the stream threshold approaches used in hydrologic analysis. *ISPRS International Journal of Geo-Information* 7, 201. https://doi.org/doi:10.3390/ijgi7060201

Rodríguez Iturbe, I., Valdés, J.B., 1979. The geomorphologic structure of hydrologic response. *Water resources research* 15, 1409-1420. https://doi.org/10.1029/WR015i006p01409

Romero Díaz, M.A., López Bermúdez, F., 1987. Morfometría de redes fluviales: revisión crítica de los parámetros más utilizados y aplicación al Alto Guadalquivir. *Papeles de Geografía* 12, 47-62.

Scian, B., 2000. Episodios ENSO y su relación con las anomalías de precipitación en la pradera pampeana. *Geoacta* 25, 23-40.

Schumm, S.A., 1956. Evolution of drainage systems and slopes in badlands at Perth Amboy, New Jersey. *Geological society of America bulletin* 67, 597-646. https://doi.org/10.1130/0016-7606(1956)67[597:EODSAS]2.0.CO;2

Shekar, P.R., Mathew, A., 2024. Morphometric analysis of watersheds: a comprehensive review of data sources, quality, and geospatial techniques. *Watershed Ecology and the Environment* 6, 13-25. https://doi.org/10.1016/j.wsee.2023.12.001

Tarboton, D.G., Bras, R.L., Rodriguez Iturbe, I., 1991. On the extraction of channel networks from digital elevation data. *Hydrological Processes* 5, 81-100. https://doi.org/10.1002/hyp.3360050107

Thompson, J.A., Bell, J.C., Butler, C.A., 2001. Digital elevation model resolution: effects on terrain attribute calculation and quantitative soil-landscape modeling. *Geoderma* 100, 67-89. https://doi.org/10.1016/S0016-7061(00)00081-1

USACE, 2023, *Hydrologic Modeling System HEC-HMS User's Manual* Hydrologic Engineering Center, U.S. Army Corps of Engineers, Davis, CA, USA.

Volonté, A., Gil, V., 2023. Diagnóstico y monitoreo de ambientes fluviales a partir de geoindicadores. Cuenca del Oro (Argentina). *Cuadernos Geográficos* 62, 130-149. https://doi.org/10.30827/cuadgeo.v62i1.25343

Wang, Y.-J., Qin, C.-Z., Zhu, A.-X., 2019. Review on algorithms of dealing with depressions in grid DEM. *Annals of GIS* 25, 83-97. https://doi.org/10.1080/19475683.2019.1604571

Wu, M., Shi, P., Chen, A., Shen, C., Wang, P., 2017. Impacts of DEM resolution and area threshold value uncertainty on the drainage network derived using SWAT. *Water SA* 43, 450-462. https://doi.org/10.4314/wsa.v43i3.10

Wu, S., Li, J., Huang, G.H., 2008. A study on DEM-derived primary topographic attributes for hydrologic applications: Sensitivity to elevation data resolution. *Applied Geography* 28, 210-223. https://doi.org/10.1016/j.apgeog.2008.02.006

Zapperi, P., Casado, A., Gil, V., Campo, A.M., 2006. Caracterización de las precipitaciones invernales en el Suroeste bonaerense. In: N. Cazzaniga, M. Vaquero (Eds.), *Ambiente natural, campo y ciudad: Estrategias de uso y conservación en el Sudoeste Bonaerense*. Ediciones UNS, Bahía Blanca, pp. 63-68.

Zapperi, P., Ramos, B., Gil, V., Campo, A.M., 2007. Caracterización de las precipitaciones estivales en el Suroeste bonaerense. In: *Contribuciones Científicas*. GAEA, Posadas, pp. 483-491.

Zavoianu, I., 1985. *Morphometry of drainage basins. Serie 20: developments in water science.* Elsevier, Amsterdam, Neederlands.